

FABRICATION AND MECHANICS OF NANORODS

Hanchen Huang

Department of Mechanical, Aerospace and Nuclear Engineering, Rensselaer Polytechnic Institute, Troy, NY 12180, USA

Received: August 10, 2006

Abstract. This paper presents physics based design of nanorods, and mechanical deformation of such nanorods. Our study relies on primarily atomistic simulations, and the final results are corroborated by accompanying experiments. The design starts from understanding of three pieces of fundamental physics: geometrical shadowing during physical vapor deposition, twin formation during growth, and three-dimensional Ehrlich-Schwoebel barriers. The integration of these three pieces leads to the design of selforganized branching of nanorods. Due to the large surface-to-volume ratio, both elastic and plastic deformations of nanorods or nanoplates are distinctive from their bulk crystals. Our atomistic simulations show that Young's moduli of nanoplates can be larger or smaller than their bulk counterparts. The variation is a result of competition among bonds loss and bond saturation at surfaces, and bulk nonlinear elasticity. Further, at nanoscale, anomaly of dislocation glide is possible.

1. INTRODUCTION

Nanostructured materials are the enabling block of nanotechnology, and discovery of such materials by design is therefore critically important. The nanostructured materials can be zero dimensional such as quantum dots, one dimensional such as nanowires, two dimensional such as nanoplates. Although it is possible to manipulate individual atoms [1], such manual manipulation is not feasible for mass production of nanostructured materials. It is physics based self-assembly that may provide the mass production for nanotechnologies.

Nanostructured materials are distinctive from bulk materials in terms of their electronic, electrical, optical, thermal, magnetic, and mechanical properties. In bulk crystals, standard handbooks provide elastic constants in the form of C_{ij} , which do not vary from one crystal to another. At the nanoscale, the elastic constants become variable. For example, Young's moduli of nanoplate may increase or decrease as size changes.

This paper presents physics based design of nanorods and shows how and why their mechanical properties depend on size.

2. PHYSICS BASED DESIGN OF NANORODS

This section begins with the understanding of three pieces of fundamental physics, and proceeds to the design of branched nanorods, to computer simulations, and to experimental validations.

The first piece of fundamental physics is geometrical shadowing in physical vapor deposition. When atoms approach substrate from a source – sputtered target or evaporation source in vacuum – their trajectories are approximately straight, as shown in Fig. 1. Under the glancing angle deposition, the angle θ between the incident direction and the vertical axis is close to 90° . Mounds develop as a result of insufficient diffusion or strain energy, for example. The peak areas receive more deposited atoms, and valley areas receive less, since the incident atoms follow straight lines. The shaded light-

Corresponding author: Hanchen Huang, e-mail: hanchen@rpi.edu

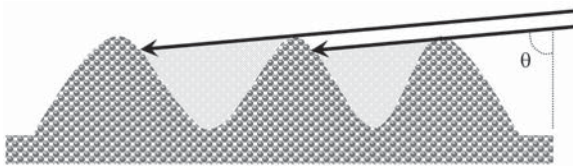


Fig. 1: Schematic of geometrical shadowing.

Fig. 1. Schematic of geometrical shadowing.

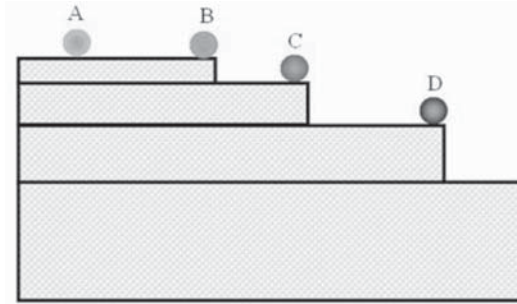


Fig. 3. Schematic of adatom diffusion on flat surface and down steps.

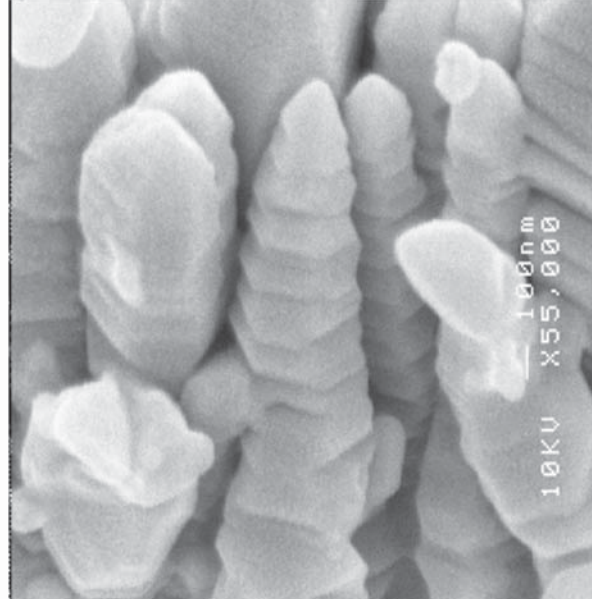
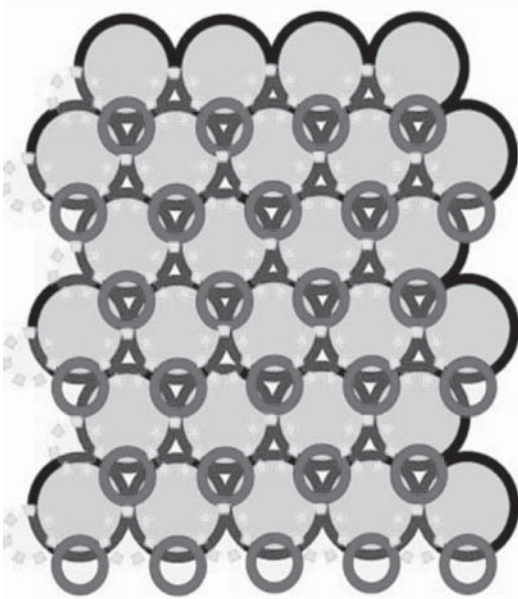


Fig. 2. (a) Stacking ABCABCABC in FCC crystal, with large circles on A layer, small circles on B layer, and small open circles on C layer; (b) Scanning electron microscopy image of Cu $\langle 111 \rangle$ nanorods.

gray areas in Fig. 1 will receive no direct deposition. Without sufficient diffusion, the shaded areas will not grow. As a result, the peaks grow taller, and the valleys become deeper. The growing peaks develop into columns or rods, as deposition continues. This growth mode is the core of the so-called Glancing Angle Deposition [2].

The second piece of fundamental physics is the formation of stacking fault or growth twin. During the growth of face-centered-cubic (FCC) metal thin films, a $\langle 111 \rangle$ out-of-plane texture usually develops; that is, they have $\{111\}$ planes parallel to the substrate. On this plane, atoms are close packed. In FCC, the closed packed planes are stacked in the order of ABCABCABC, as shown in Fig. 2a. An alternative stacking is ABABABAB, which leads to

hexagonal-close-packed (HCP) structure. In FCC, if a local stacking order of HCP appears, a stacking fault forms. During the growth, one $\{111\}$ layer may be at the HCP stacking, and subsequent layers follow the FCC stacking; this particular $\{111\}$ layer becomes a twin boundary. The formation of twin boundaries leads to the zigzag shape of $\langle 111 \rangle$ nanorods, as shown in Fig. 2b [3].

The third piece of fundamental physics is surface diffusion. As thin films or nanorods grow, $\{111\}$ surface facets develop (cf. Fig. 2b). The dimension of such facets is usually on the order of 200 nm, and it depends on surface diffusion and atoms clustering. As an order of magnitude estimate, the diffusion distance of adatoms is a good approximation of the surface facets dimension. Based on the diffu-

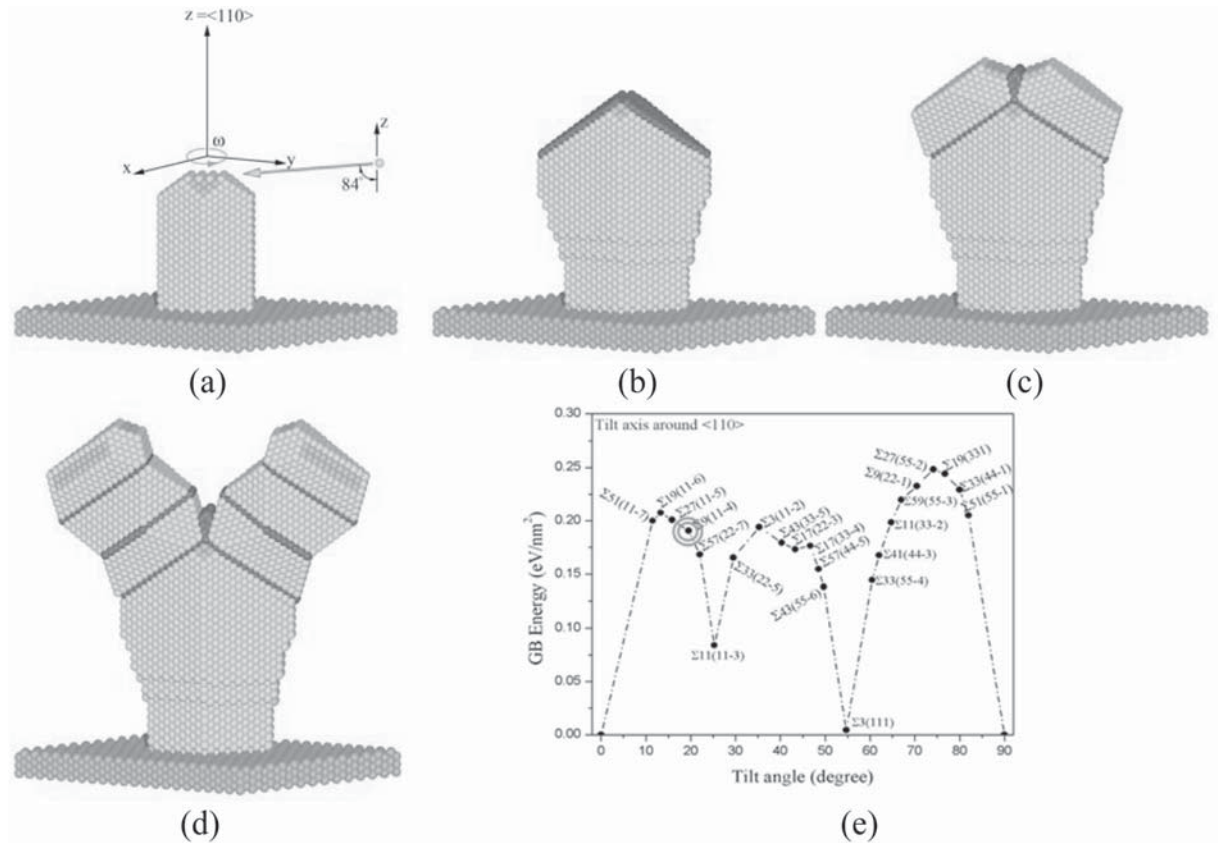


Fig. 4. Conceptual design of nanorods branching (a-d), and grain boundary (GB) formation energy showing high energy GBs vs low energy $\Sigma 3$ twin GB.

sion barrier of adatoms on flat surface, the diffusion distance is on the order of 100,000 nm; the lifetime of an adatom is taken to be the time of depositing one monolayer of atoms. Even taking the conventional Ehrlich-Schwoebel barrier into account, this distance is still on the same order of magnitude, which is about 1000 times larger than the experimental value. In 2002, our group realized that the diffusion barrier between two facets was much larger than the surface diffusion barriers recognized earlier, and termed this barrier three-dimensional Ehrlich-Schwoebel (3D ES) barrier [4]. As shown in Fig. 3, an adatom on flat surfaces (A) may experience small diffusion barrier. As an adatom steps down a monolayer step (B), the barrier increases by the amount of Ehrlich-Schwoebel barrier. As the step height goes up to two (c) or three (d) atomic layers, the adatom essentially diffuses between two facets, and the diffusion barrier may go up substantially. As an example, the diffusion barrier of an adatom on flat {111} surface in Cu is only 0.04 eV,

and the 3D ES barrier is at least 0.30 eV [5]. For small mobile clusters, the 3D ES barrier is also much larger than that on flat surfaces [6]. Based on the barrier of 0.30 eV, the diffusion distance of an adatom under typical physical vapor deposition conditions is about 200 nm. Finally, with the understanding of the 3D ES barrier, we are able to explain why surface facets are 200 nm, instead of 100,000 nm, in dimension.

With the understanding of the three pieces of fundamental physics, we are now ready to integrate them in designing nanorods. When FCC nanorods grow, it is common that they are <110> textured; that is, their {110} planes are parallel to the substrate. Therefore, the starting point of our conceptual design is <110> FCC nanorods, as shown in Fig. 4a. Using the glancing angle (say 84°) deposition, we take the advantage of geometrical shadowing to enhance nanorods growth, in contrast to the growth of uniform films. As deposition proceeds, single atomic layer may take fault stacking, indi-

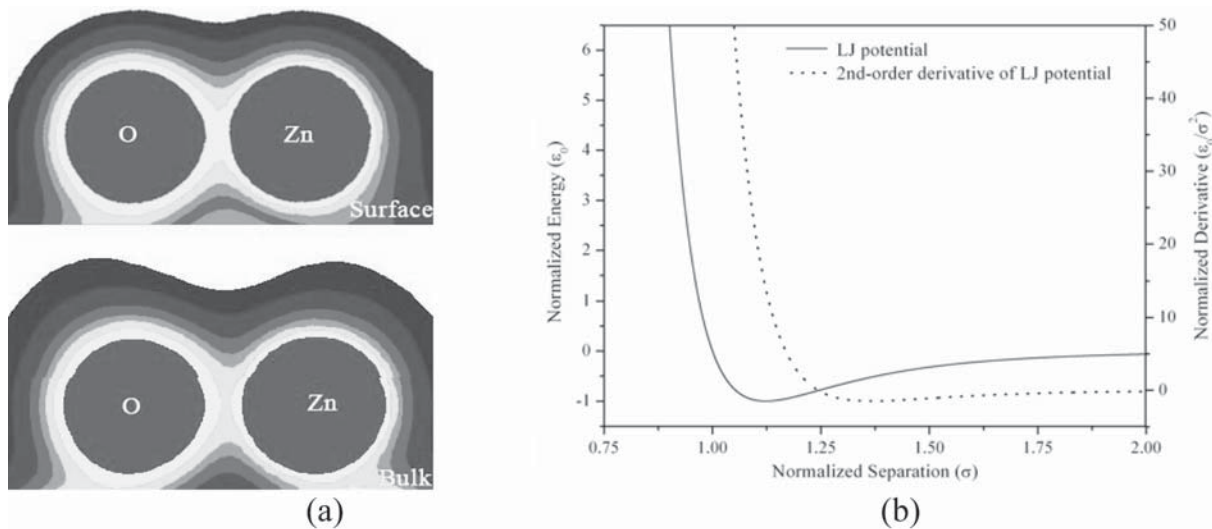


Fig. 5. (a) Electron density distribution along a bulk bond and a surface bond in ZnO; (b) energy and curvature as a function of atomic separation according to Lennard-Jones (LJ) potential.

cated by the red spheres in Fig. 4b; the single fault layer is a twin boundary. When the two twin boundaries meet, they form a high-energy $\Sigma 9$ grain boundary, as Fig. 4e shows [7]. Energetically, atoms prefer single crystalline sites than $\Sigma 9$ GB sites. As a result, bifurcation starts and the nanorod branches (Fig. 4d). Due to the 3D ES barrier, the facets will not grow too large, ensuring the bifurcated nanorod to branch out. Continued growth will lead to Y-shaped nanorod of Fig. 4e, due to the combination of geometrical shadowing, twin boundary formation, and 3D ES barrier.

Taking this conceptual design one step further, we have studied the growth process using molecular dynamics simulations. Indeed, the simulation results confirm that the conceptual design is valid [8]. Further, the ensuing experiments of Gall and associate have validated the conceptual design and the molecular dynamics simulations.

3. MECHANICAL PROPERTIES

Nanostructured materials, such as nanorods, are distinctive from bulk crystals in terms of mechanical properties: both elastic and plastic properties. In discussing elastic properties, we concentrate on nanoplates instead of nanorods, in order to clearly separate effects of different surfaces and ridges. The Young's moduli of nanoplates are size dependent,

and this dependence is a result of the large surface-to-volume ratio.

At surfaces, atoms lose some bonds. As a result, the Young's moduli will be smaller than bulk values. At the same time, two other factors make the Young's moduli larger than bulk values. First, the bond order effects make surface atomic bonds stronger than bulk bonds; this is a concept used in developing interatomic potentials [9], and also employed in representing surface energies [10]. The phenomenon of surface bond saturation is shown in Fig. 5 [11]. The electron density along a surface bond, particularly near the middle point, is substantially higher than that along a bulk bond (Fig. 5a). The higher electron density results in stronger surface bonds. This effect increases the Young's moduli of nanoplates, with respect to bulk values. Second, the bulk nonlinear elasticity may also contribute to the increase of Young's moduli. The nonlinearity is demonstrated using the Lennard-Jones potential in Fig. 5b. The curvature, or the second order derivative of energy with respect to separation, increases as atomic separation decreases. Under surface stress, nanoplates may contract or expand. If the contraction dominates, the atomic separation decreases and the interior of a nanoplate may have larger Young's moduli due to the nonlinearity. Our recent studies have shown that the competition of surface bond saturation and bulk nonlinear elastic-

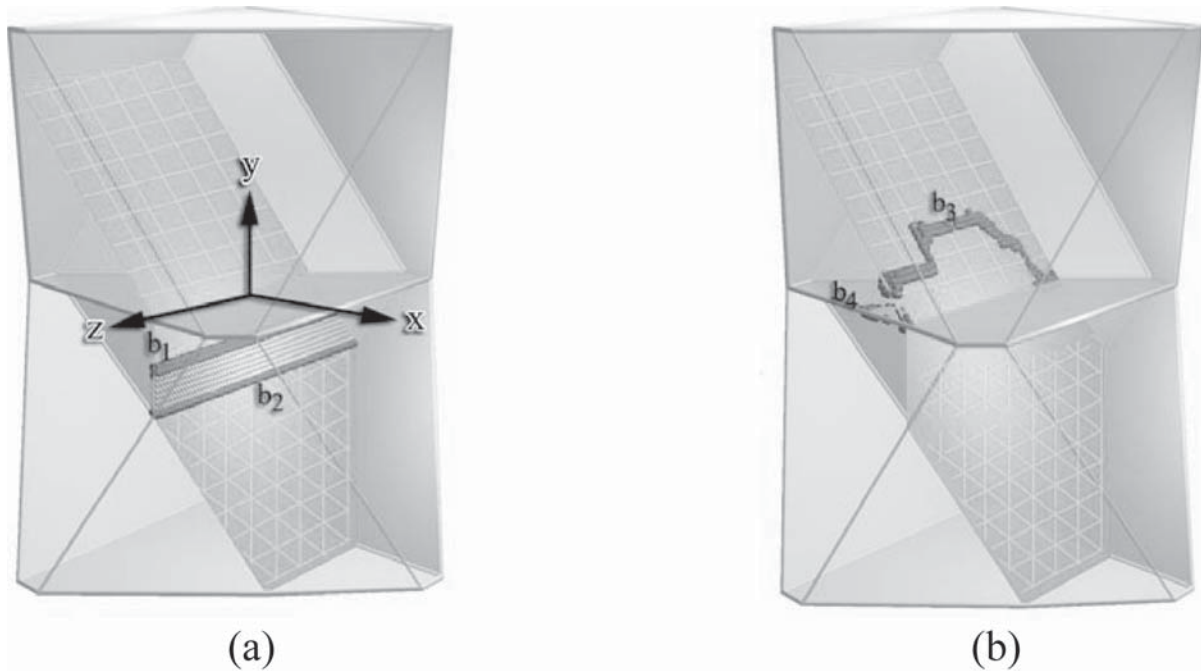


Fig. 6. A complete dislocation consisting of two Shockley partial dislocations on Cu{111} glide plane (a), and a complete dislocation on Cu{100} after penetrating a twin boundary (b).

ity, together with the bond loss at surfaces, determines whether Young's moduli of nanoplates are larger or smaller than their bulk counterparts [12–15]. When surface reconstruction is possible, it also affects the degree of surface bond saturation [14].

Beyond elastic deformation limit, nanorods deform plastically. One well known plastic deformation mechanism of nanorods is the nucleation of dislocations from surfaces and subsequent glide [16]. With the presence of twin boundaries (Fig. 3), another novel deformation mechanism is possible. As shown in Fig. 6, a complete dislocation on Cu{111} approaches a twin boundary under axial loading, and glides on Cu{100} plane after penetrating the twin boundary. This process also leaves a partial dislocation on the twin boundary. The glide on {100} maximizes the accommodation of plastic strain along the loading direction, and the nucleation is facilitated by the surface–twin boundary intersection. It should be emphasized that the anomaly is a possibility, instead of generality. As the dimension of the nanorods increases, even nominal axial loading may lead to three dimensional stress states inside the nanorods. Consequently, non-axial stress components may favor normal {111} dislocation glides.

4. SUMMARY

This paper presents physics based design of nanorods self-assembly, particularly self-assembled branching into Y-shapes. This design is made possible through (1) understanding of three pieces of fundamental physics, (2) integration of the understanding into conceptual design, and (3) atomistic simulations of the conceptual design. The subsequent experimental validation of the conceptual design of the simulations adds to confidence in such design.

Further, the paper presents the elastic and plastic deformation behaviors of nanorods and nanoplates. The Young's moduli of nanoplates may increase or decrease with size, as a result of competition among surface bond saturation, bond loss near surfaces, and bulk nonlinear elasticity. During plastic deformation of twinned FCC nanorods, anomalous {100} dislocation glide, in addition to normal {111} glide, is possible.

ACKNOWLEDGEMENT

This paper is based on works done by the author's associates/students over the past few years; they include Dr. Jian Wang, Dr. Longguang Zhou, Dr. Helin Wei, Dr. Shaojun Liu, Dr. Lixin Zhang, Dr. Alberto Coronado, and Mr. Hyun Woo Shim. The author also acknowledges financial support from Basic Energy Science of Department of Energy (DE-FG02-04ER46167), and National Science Foundation (CMS-0409476 and DMI-0423358).

REFERENCES:

- [1] G. K. Binnig, *U.S. Patent 4724318* (1988).
- [2] K. Robbie, M. J. Brett and A. Lakhtakia // *Nature* **384** (1996) 616.
- [3] H. Huang, H. L. Wei, C. H. Woo and X. X. Zhang // *Appl. Phys. Lett.* **81** (2002) 4359.
- [4] S. J. Liu, H. Huang and C. H. Woo // *Appl. Phys. Lett.* **80** (2002) 3295.
- [5] J. Wang, H. Huang and T S. Cale // *Model. Simul. Mater. Sci. Eng.* **12** (2004) 1209.
- [6] B. H. Aguilar, J. C. Flores, A. M. Coronado and H. Huang // *Model. Simul. Mater. Sci. Eng.* (2006), submitted.
- [7] J. Wang, Ph.D dissertation (Rensselaer Polytechnic Institute, Aug. 2006).
- [8] J. Wang, H. Huang, S. V. Kesapragada and D. Gall // *Nano Lett.* **5** (2005) 2505.
- [9] J. Tersoff // *Phys. Rev. Lett.* **56** (1986) 632.
- [10] H. Huang, G. H. Gilmer and T. Diaz de la Rubia // *J. Appl. Phys.* **84** (1998) 3636.
- [11] L. X. Zhang and H. Huang // *Appl. Phys. Lett.* (2006), submitted.
- [12] L. G. Zhou and H. Huang // *Int. J. Multi. Comp. Eng.* **4** (2006) 19.
- [13] H. Y. Liang, M. Upmanyu and H. Huang // *Phys. Rev. B* **71** (2005) 241403.
- [14] H. W. Shim, L. G. Zhou, H. Huang and T. S. Cale // *Appl. Phys. Lett.* **86** (2005) 151912.
- [15] L. G. Zhou and H. Huang // *Appl. Phys. Lett.* **84** (2004) 1940.
- [16] J. Wang and H. Huang // *Appl. Phys. Lett.* **88** (2006) 203112.